CHARLES UNIVERSITY

Faculty of Science

Study programme: Clinical and Toxicological Analysis

Branch of study: Clinical and Toxicological Analysis

Shannelle Diana Habániková

Electrochemical oxidation of selected bile acids in acetonitrile
Elektrochemická oxidace vybraných žlučových kyselin v acetonitrile

Bachelor´s thesis

Supervisor: RNDr. Karolina Schwarzová, Ph.D

Prague, 2017

This bachelor thesis was financially supported by the Grant Agency of the Charles University (project GAUK 1440217).

Prohlášení

Prohlašuji, že jsem tuto závěrečnou práci zpracovala samostatně a že jsem uvedla všechny použité informační zdroje a literaturu. Tato práce ani její podstatná část nebyla předložena k získání jiného nebo stejného akademického titulu.

Jsem si vědoma toho, že případné využití výsledků, získaných v této práci, mimo Univerzitu Karlovu v Praze je možné pouze po písemném souhlasu této univerzity.

V Praze dne 1. května 2017.

Abstract

The concentration of bile acids is an important parameter in hepatobiliary tract diseases. This work deals with the electrochemical oxidation of the chenodeoxycholic (CDCA) and cholic acid (CA) at boron dopped diamond (BDD) electrode in comparison with the oxidation at glassy carbon (GCE) and platinum electrode (PtE), in a mixed environment of acetonitrile and water (0.26 % from 0.1 $mol \cdot l^{-1}$ $HClO_4$, supporting electrolyte). The measurement was carried out in an electrochemical cell with salt bridge containing 0.5 $mol \cdot l^{-1}$ $NaClO_4$ separating the working and the Pleskov´s reference electrode (0.01 $mol \cdot l^{-1}$ $AgNO_3$ and 1 $mol \cdot l^{-1}$ $NaClO_4$ in acetonitrile). Cyclic voltammetry (CV) characterization of BDD electrode by a redox pair $[Fe(CN)_6]^{4-/3-}$ (c = 0.1 $mmol \cdot l^{-1}$) in 1 $mol \cdot l^{-1}$ KCl was performed. Quasi-reversible behaviour was observed and the difference of the anodic and the cathodic peak potential ranged from 80 to 200 mV, depending on the scan rate. Alumina polishing (4 min) of the BDD electrode was identified as the most appropriate method of activating the surface and it was applied between consecutive voltammetric scans in the presence of CA and CDCA. Irreversible anodic peaks of CDCA and CA in acetonitrile-water (0.26 %) were observed at the relatively high potentials of about +1100 ± 100 mV, depending on the scan rate and used voltammetric technique. This observation was noted only in CA and CDCA, both of which contain 7-α-hydroxy group, not for the other teste bile acids (deoxycholic, lithocholic acid). According to the linear dependency of peak current to square root of the scan rate, it can be seen that the oxidation process is controlled by diffusion. The calibration dependences were measured at a concentrations range of 1 - 900 $\mu mol \cdot l^{-1}$ CDCA and CA 1 - 90 $\mu mol \cdot l^{-1}$, they are linear and reach higher sensitivity at BDD in comparison to GC and Pt electrodes. Further studies will be devoted to the oxidation mechanism and the possibility of its use for selective detection of these bile acids.

Key words

cyclic voltammetry, differential pulse voltammetry, electrochemical oxidation, boron doped diamond electrode, glassy carbon electrode, platinum electrode, chenodeoxycholic acid, cholic acid

Abstrakt

Koncentrace žlučových kyselin je důležitým parametrem v onemocněních hepatobiliárního traktu. Tato práce se zabývá elektrochemickou oxidací kyseliny chenodeoxycholové (CDCA) a cholové (CA) na borem dopované diamantové elektrodě (BDD) v porovnání s oxidací na skelném uhlíku (GCE) a platině (PtE), ve směsném prostředí acetonitrilu a vody (0.26 % z $HClO_4$, základný elektrolyt). Měření bylo provedeno v elektrochemickém článku se solným můstkem obsahujícím 0.5 $mol \cdot l^{-1}$ $NaClO_4$, který oddělil pracovní a Pleskovovu referenční elektrodu (0.01 $mol \cdot l^{-1}$ $AgNO_3$ a 1 $mol \cdot l^{-1}$ $NaClO_4$ v acetonitrilu). Charakterizací BDD elektrody (nejširší potenciálový okno v anodické oblasti) pomocí cyklické voltametrie a redoxního markeru $[Fe(CN)_6]^{4-/3-}$ (c = 0.1 $mmol \cdot l^{-1}$) v 1 $mol \cdot l^{-1}$ KCl, bylo zjištěno kvasi-reverzibilní chování a rozdíl anodického a katodického potenciálu byl v rozmezí od 80 do 200 mV (v závislosti na rychlosti polarizace). Leštění BDD elektrody na alumině (4 minuty) bylo identifikováno jako nejvhodnější metoda aktivace jejího povrchu a byla aplikována mezi voltametrickými skenmi v přítomnosti CA a CDCA. Ireverzibilní anodické píky oxidace CDCA a CA v prostředí acetonitril-voda (0.26 %) byly pozorovány při poměrně vysokém potenciálu přibližně +1100 ± 100 mV, v závislosti na rychlosti polarizace a použité voltametrické technice. Toto pozorování bylo zaznamenáno pouze u CA a CDCA, které obě obsahovaly 7-α-hydroxy skupinu, ostatní studované žlučové kyseliny (deoxycholová, litocholová kyselina) voltametrickou odezvu neposkytují. Podle závislosti proudu píků na odmocnině z rychlosti polarizace lze vidět, že oxidační proces je řízen difúzí. Kalibrační závislosti, které byly měřeny v rozmezí koncentrací 1 – 90 $\mu mol \cdot l^{-1}$ CA a CDCA, jsou lineární a nejvyšší citlivosti bylo dosáhnuto u BDD (měla nejvyšší poměr signálu k pozadí) ve srovnání s elektrodami GCE a PtE. Další studie budou věnovány oxidačnímu mechanismu a možnosti jeho použití pro selektivní detekci těchto žlučových kyselin.

Klíčová slova

cyklická voltametrie, diferenční pulzní voltametrie, elektrochemická oxidace, borem dopovaná diamantová elektroda, elektroda ze skelného uhlíku, platinová elektroda, kyselina chenodeoxycholová, kyselina cholová

Acknowledgement

I am deeply grateful to my supervisor RNDr. Karolina Schwarzová, Ph.D. for her invaluable support throughout this work, willingness and responsiveness and for her detailed and constructive advice and comments.

I wish to extend my warmest thanks to Mgr. Jan Klouda and all who have helped me with my work. Big thanks belongs to all colleagues from the laboratory for their advice and creation of excellent working environment, especially Ing. Ján Tarábek, Ph. D.

I owe my thanks to my parents, my partner and my closest friends for their loving support during my study, their encouragement and appreciation.

Abbreviations

BDD	Boron doped diamond
c	Concentration
CA	Cholic acid
cAMP	Cyclic adenosine monophosphate
CDCA	Chenodeoxycholic acid
CEC	Capillary electrochomatography
CMC	Critical micellization concentration
CMpH	Critical micellization pH
CV	Cyclic voltammetry
CZE	Capillary zone electrophoresis
DPV	Differential pulse voltammetry
ED	Electrochemical detection
E_p	Peak potential
FXR	Farnesoid X receptor
GCE	Glassy carbon electrode
HPLC	High-performance liquid chromatography
I_p	Peak current
LOD	Limit of detection
LOQ	Limit of quantification
MS	Mass spectrometry
pK_a	The negative decadic logarithm of the ionization constant (Ka) of an acid
PtE	Platinum electrode
RSD	Relative standard deviation
t	time
UDCA	Ursodeoxycholic acid

Content

Prohlášení 2
Abstract 3
Key words 3
Abstrakt 4
Klíčová slova 4
Acknowledgement 5
Abbreviations 6
Introduction 8
2 Theoretical part 9
2.1 Studied analytes – the bile acids 9
2.1.1 Brief history 9
2.1.2 Chemistry and biology of bile acids and salts 10
2.1.2 Physico-chemical properties of selected bile acids 13
2.2 Analytical methods for determination of bile acids 14
2.2.1 Electroanalytical methods and detectors 15
3 Experimental 18
3.1 Studied analytes and reagents 18
3.2 Apparatus, software and data analysis 18
3.3 Procedures and methods 19
3.3.1 Cyclic voltammetry 19
3.3.2 Differential pulse voltammetry 20
4 Results and discussion 21
4.1. Electrochemical characterisation of BDD electrode 21
4.2. Cyclic voltammetry of CDCA and CA on BDD electrode 25
4.3 Calibration dependences 31
5 Conclusion 37
References 39

Introduction

Bile acids were for a long time mysterious substances used in Chinese medicine to treat various biliary and gall bladder conditions. In recent years scientist revealed many new facts linked to their function in an organism, and also their therapeutic and diagnostic uses. High performance liquid chromatography is the most used method for determination of bile acids. However, UV detection is problematic because of absent double bond and therefore low absorbance. Fluorescent detection is possible just after derivatization. Mass spectrometric (MS) detection is used, which is financially, instrumentally and personally demanding. That is the reason why necessity of studying diverse easier and faster new methods for their identification and quantitation in biological matrices arose.

This bachelor thesis is part of a larger project, which aims to study the electrochemical behavior of natural steroid compounds without or with isolated double bonds at the steroid nucleus. Among them, cholesterol, phytosterols or bile acids are investigated to gain better insight into their supramolecular and conjugate interactions. The project main objective is using electrochemical oxidation and reduction of steroid compounds in electroanalysis.

The aim of this bachelor thesis was to compare the electrochemical oxidation of chenodeoxycholic acid (CDCA) and cholic acid (CA) on boron doped diamond (BDD), glassy carbon (GCE), and platinum electrodes (PtE), in context with cited literature. Cyclic voltammetry (CV) was used to study the electrochemical processes ongoing at the electrodes and an electroanalytical methods based on differential pulse voltammetry (DPV) were developed for quantitation of CDCA and CA.

2 Theoretical part

In this chapter, all important background knowledge covering the topic is going to be introduced. The first part is devoted to the general characteristics of studied chemicals, from their structure, through functions, to their physico-chemical properties. Secondly, a small insight into history and possibilities of their chemical and more specifically electrochemical analysis is given.

2.1 Studied analytes – the bile acids

2.1.1 Brief history

The journey of bile acid research started very early in the 20th century when Heinrich Wieland, then professor in Munich, persuaded his cousin´s pharmaceutical company to begin the isolation and marketing of CA from ox bile and for the first time it became easily available to the scientific community[1]. From then on, the research on bile acids had many ups and downs, because of gaining and losing popularity of therapeutical use. Nonetheless, it led to several Nobel prizes, specifically Wieland alone was awarded the 1927 Nobel Prize for his vision of CA structure[1,2]. In 1932 Desmond Bernal decided to use X-ray diffraction for studying ergosterols[1,3], his discoveries initiated wide structure related research and it later lead to confirmation of bile acid structure[1,4].

After the Second World War, the development of liquid scintillation and chromatography made biochemistry of bile acids measurable. Thanks to that, Swedish Karolinska institutet, Bengt Borgström´s group of scientist revealed some of the metabolic pathway of bile acids[1,5] and distinguished primary bile acids (made in the liver from cholesterol) from secondary bile acids (made from primary bile acids by intestinal bacteria)[1,6]. They also elucidated kinetics of their metabolism in human[1,7]. After these identifications, there were several attempts of using bile acids therapeutically (gallstone dissolution[1,8]), but after the development of laparoscopic cholecystectomy in the 1990s, bile acids were again thought to have little medical value. Nowadays they again started to gain popularity, when they appeared in a completely new light representing signal molecules, which opens a whole new chapter of molecular biology[1].

2.1.2 Chemistry and biology of bile acids and salts

Bile acids are soluble catabolites derived from cholesterol (Fig. 2.1). They are amphipatic molecules, with four steroid rings, marked A to D, from left to right[9]. They contain end carboxyl group on their side chain and have one to three hydroxyl groups, situated on the third, and then on the seventh, and/or twelfth carbon. These hydroxyl groups lie below concave plane of rings in alpha orientation and attached methyl groups lie above the convex plane in beta orientation. This orientation means that the acid molecules have a polar and non-polar face, which leads to formation of micelles and facilitates the digestion and absorption of dietary lipids and fat-soluble vitamins from the small intestine. Furthermore, their arrangement can differ by stereochemistry of A/B ring juncture or presence of unsaturation, or the site of ending carboxyl group, which can be amidated with taurine or glycine. The structure of chenodeoxycholic acid can be found in the Figure 2.2 and structure of cholic acid in the Figure 2.3, together with hydroxyls of other bile acids.

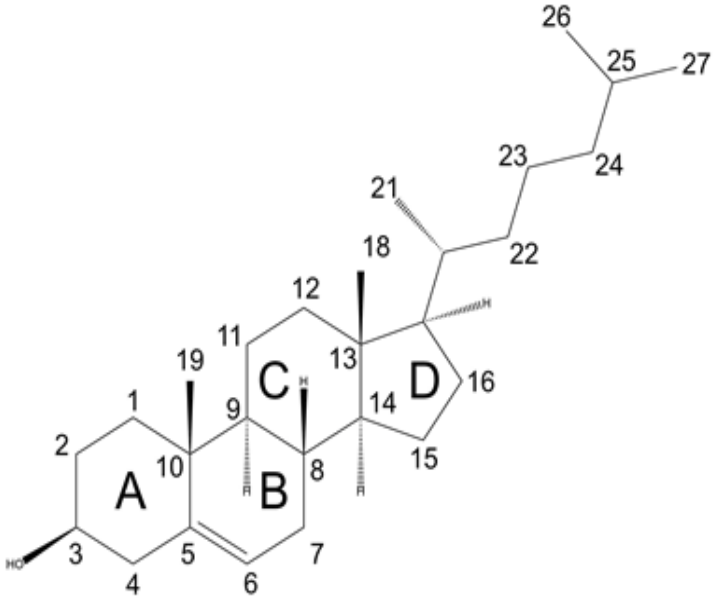

Fig. 2.1 Structure of cholesterol with original numbering system from 1930s when it was first published and with labelled steroid rings as described above[10,11].

Two major groups of bile acids are distinguished by their five or eight carbon side chain on steroid rings at C_{17}[10,11]. Those with 24-carbon atoms in the skeleton, termed cholanoic acids and those with 27-carbon atoms, termed cholestanoic acids. Common bile acid names are considered "grandfathered" and are used as building blocks for other trivial names, usually composed of the term "cholic", that also refers to 3α, 7α, 12α -trihydroxy-5-cholan-24-oic acid, following the 1930s numbering system (Fig. 2.2), but also 24 carbon cholanoic acid skeleton and a prefix referring to

the pattern of hydroxyl substituents, named after the animal species from which it was originally isolated, for example urso- (*Ursus* – bear from latin), muri- (*Mus* – mouse from latin), hyo- (Huoeidēs – pig from ancient greek), cheno- (Khēn – goose from ancient greek) *etc.*

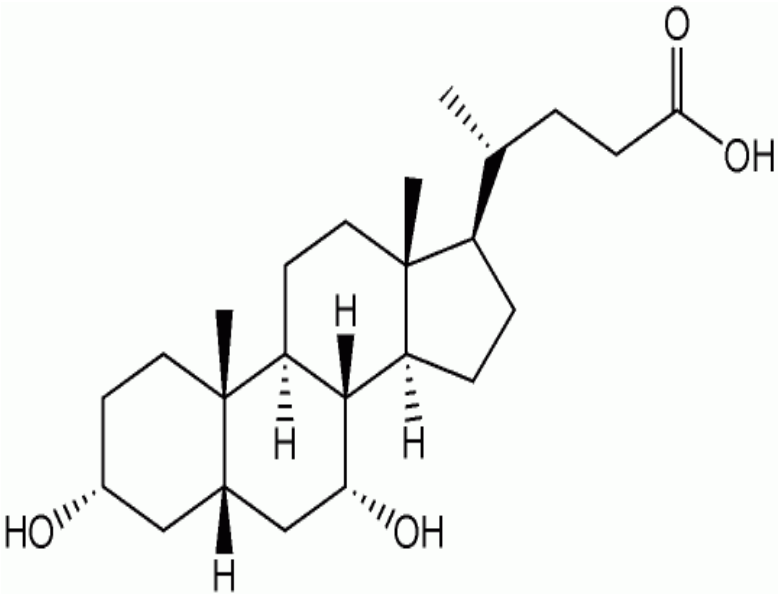

Fig. 2.2 Frontal view of CDCA with stereochemistry

Synthesis (Fig. 2.3) of normal cholanoic acid takes place in the liver, where this process has 17 steps, proceeding in multiple organelles[10]. The pathway involves insertion of hydroxyl groups at C^7 and C^{27} on cholesterol that leads to oxidation of cholesterol´s B ring, followed by further reduction of side chain by three carbons occurs and finally carboxyl group is added[9,10]. The most common resulting bile acids are CA and CDCA that depends on 12-hydroxylation of the steroid ring, which by its classification belong to primary bile acids[11]. Secondary bile acids are then formed by bacterial modification. These include for example deoxycholic, lithocholic, and ursodeoxycholic acid.

When talking about bile acids, it is important to mention bile salts that are their glycine or taurine conjugates found in the liver excreted bile[9]. Just before the acids leave the liver, they are conjugated via bond between the carboxyl group of bile acid and amino group of glycine or taurine. Three times more glycine than taurine conjugated bile salts are formed. This conjugation reduces pK_a of carboxyl group in glycine, and sulphonate group in taurine, what fully ionises the molecule and it becomes more effective detergents with more enhanced amphipathic function.

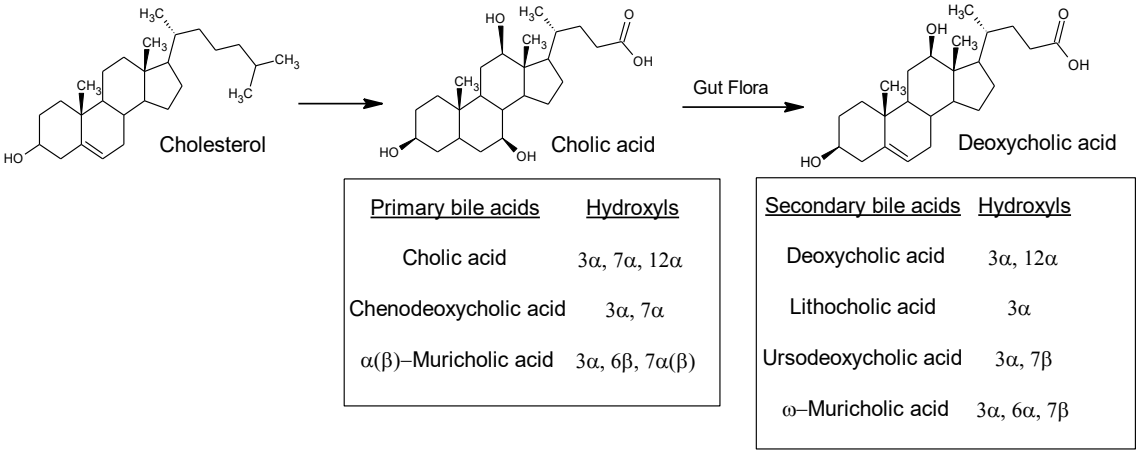

Fig. 2.3: The conversion of the 27-carbon cholesterol to primary and secondary 24-carbon bile acids by liver enzymes and the microbiome is shown. Representative primary and secondary bile acids together with the orientation of the hydroxyls are indicated[10].

It was shown that bile acids are very interesting and important substances in our body with multiple functions: Firstly, they solubilise dietary lipids and thus enhance their digestion, and absorption of fat-soluble vitamins, by formation of mixed micelles; secondly the gall bladder micelles serve to solubilize cholesterol in bile, keeping it from crystallization and gallstone formation[10]. The flow of bile is induced by bile salts and it also has bacteriostatic function. Equally importantly the bile salts participate on sterol homeostasis, by conversion of cholesterol to bile acids and the subsequent excretion. Any disruption or failure of these functions can lead to cholestasis, gallstones, inflammation, malabsorption of lipids and fat-soluble vitamins, bacterial overgrowth in the small intestine, atherosclerosis, neurological diseases and various inborn defects such as Progressive Familial Intrahepatic Cholestasis. However, the latest discoveries shown that specific bile acids differentially activate three nuclear receptors, namely farnesoid X receptor (FXR, belongs to a superfamily of transcription factors, regulates the metabolism of plasma lipoproteins, glucose, steatosis, inflammation, bacterial growth and liver regeneration, in addition to the regulation of bile acid homeostasis), pregnane X receptor (PXR, provides protection against inflammatory bowel disease by reducing expression of inflammatory cytokine) and vitamin D receptor (VDR, can modulate hepatic bile acid synthesis) and one G-protein-coupled receptor (TGR5,cell surface activation results in receptor internalization, increased cAMP levels and activation of protein kinase).

Because of above listed functions, bile acids have been used as thereapeutics, since they have become available, but with further medical and chemical development interest in them fluctuated[1]. Nowadays, at least two types of drugs, based on natural bile acids are being tested for their utility

in the treatment of liver disease. Firstly, the obeticholic acid, the 6-ethyl derivative of CDCA, FXR agonist, efficient for primary biliary cirrhosis and nonalcoholic steatohepatitis and secondly, the C_{23} homolog of ursodeoxycholic acid (UDCA), efficient for the treatment of primary sclerosing cholangitis are being tested in clinical trials[1].

2.1.2 Physico-chemical properties of selected bile acids

Arched skeleton, ten chiral carbons and hydroxyls´ ability to form hydrogen bonds make bile acids ideal compounds to study the reflection of the structural configuration to their physico-chemical properties[12], the most basic characteristics are listed in Tab 1.1. As mentioned before, bile acids are amphipathic molecules with polar and nonpolar side, which is essential for forming mixed micelles, that are responsible for most of their functions[10]. The presence or absence of hydroxyl groups in the α or β orientation at position 3, 6, 7 and 12 on the steroid rings affects both their solubility and hydrophobicity (hydrophobic to hydrophilic order: lithocholic > deoxycholic > chenodeoxycholic > cholic > ursodeoxycholic > muricholic acid). This difference is also reflected on activation of four nuclear receptors, excluding muricholic acid.

Tab. 1.1 Selected physico-chemical characteristics of CDCA and CA

	chenodeoxycholic acid[13]	cholic acid[13]
IUPAC name	(3α,5β,7α,8ξ,20R)-3,7-Dihydroxycholan-24-oic acid	(3α,5β,7α,8ξ,12α,20R)-3,7,12-Trihydroxycholan-24-oic acid
CAS registry number	474-25-9	81-25-4
Molecular formula	$C_{24}H_{40}O_4$	$C_{24}H_{40}O_5$
Molecular mass	392.572	408.571
Melting point	168 – 171 °C	198 °C
Water solubility	0.0899 mg·ml^{-1} (20 °C)	0.175 mg·ml^{-1} (20 °C)
$pKa_{1,2}$	4.6; -0.54;	4.48; -0.16;
Hydrogen donor count	3	4

In order to reveal the complexity of micellization, X-ray diffractions, surface chemistry, pH solubility, ionization behavior, and also solubilization properties of bile acids, physico-chemical properties were studied in detail and reviewed[1]. Another important parameter influencing solubility of acids is the pK_a. Those of unconjugated bile acids fluctuates around 5.1, taurine-conjugated bile acids have low pK_a values and thus they are strong acids, and glycine conjugates have pK_a about 4, so they are more likely to get ionized, caused by the electron withdrawal effect of the amide bond, which enhances the loss of a proton from the carboxyl group.

Solubilisation, one of the main functions, is concentration dependent. Critical micellization concentration (CMC) is used to define concentration point, at which solubility escalates and micelles are formed[1]. In contrast with typical detergents, micelles are formed by gradual aggregation, resulting in not strictly defined CMC, but rather a range of concentrations. Moreover, bile acid aggregates do not occur alone in nature. In fact, they form mixed micelles with a phosphatidylcholine in bile, and fatty acids in the intestines, both maintains CMC. These values for C_{24} bile acids were approximated and tabulated ranged from 9 $mmol \cdot l^{-1}$ (chenodeoxycholic acid) to 60 $mmol \cdot l^{-1}$ (ursocholic acid) in water at 25 °C[12,14]. Slightly lower values from 9 $mmol \cdot l^{-1}$ to 35 $mmol \cdot l^{-1}$ respectively in simulated physiological conditions of 0.15 $mmol \cdot l^{-1}$ Na^+ ions were reported. CMC proportionately increases with number of hydroxyl groups in the steroid molecule and conjugation with glycine or taurine results in a slight decrease. Furthermore, CMpH values stand for critical micellization pH and defines rough concentration, at which bile acids are highly soluble above it and insoluble bellow[1]. The CMpH of CDCA is about 6.8, 7.9 for UDCA, and 4.8 for glycocholate.

Above shortlisted parameters are important to understand the processes influencing detection, quantification, or even reaction mechanism to optimize analytical methods[12].

2.2 Analytical methods for determination of bile acids

The level of total bile acids sharply increases in the case of hepatobiliary diseases, for example early, acute hepatitis and the distinction of active and nonactive chronic hepatitis[15]. Therefore, total bile acid concentration is an important parameter for diagnosis. Today, there are many methods available for the determination in serum, such as radioimmunoassay, high-performance liquid chromatography (HPLC), preferably with mass spectrometry (MS)-based detection and enzymatic cycling assays.

In the past, bile acid analysis began with the development of improved chromatographic methods for separation[1,16]. After using paper chromatography back in the 1940s, gas-liquid partition chromatography (GLC) was developed, and its combination with mass spectrometry (GLC-MS). This method, however, lost its importance with the advances of liquid chromatography in combination with mass spectrometry (LC-MS) and tandem mass spectrometry (LC-MS / MS), which is more sensitive. Thin layer chromatography (TLC) was also used, either with normal or

reverse phase (RP-TLC). The disadvantage of this method lay in the inability to distinguish taurine and glycine conjugates from each other[1,16].

HPLC was developed in the 1970s and is used until now, usually with reverse phase mode, with C_{18} or C_8 alkyl-bonded silicic acid as the lipophilic solid phase. However, HPLC-MS / MS is the most common method for determining cholic, deoxycholic, ursodeoxycholic, lithocholic and glycocholic acid, the bile acid profiles in women suffering from primary cholestasis of pregnancy[1,17]. In fact, various detectors are used, for example UV and fluorescent detector, but they are not very reliable with regard to selectivity, because of series of pre-analytical steps, hydrolysis and derivatization. HPLC methods based on electrochemical detection modes are mentioned in the next chapter 2.2.1.

Besides HPLC, capillary zone electrophoresis (CZE), that requires less sample and solvent, can be used for determination of bile acids[18]. New miniaturized technique, capillary electrochromatography (CEC) with isocratic elution, the method that comprises benefits of both, HPLC and CZE, was created. This was innovated into pressure capillary electrochromatography (PCEC) with laser-induced fluorescence detection (LIF) at $\lambda_{ex}/\lambda_{em}$ = 473 nm/530 nm of derivatized bile acids with 4-nitro-7-N-piperazino-2,1,3-benzoxadiazole, forming a fluorescent amide[18].

However, the above mentioned methods are not flawless and new ideas for detection of bile acids and salts in complex matrices have to be presented[12,15]. In HPLC, there is a problem with the complicated procedure of derivatization and hydrolysis of bile acids, Thus, enzymatic cycling assay is the most commonly used method in clinics, in spite of great reagent consumption and low sensitivity. In the case of radioimmunoassay, there is a radioactive contamination. On behalf of the above concerns, there is an ambition to develop methods that require low amounts of reagents and solvent s, simpler operation, lower costs and higher sensitivity. One of the possible answers lies in electrochemical measurement that has many advantages such as low investment and running cost, relatively fast speed, high sensitivity, and capability of miniaturization.

2.2.1 Electroanalytical methods and detectors

Utilization of electroanalytical methods proves to be less expensive and difficult for realization[12,15]. There is not much knowledge concerning electrochemical activity of sterols including bile acids. They were reviewed recently[12,19]. The problem is that the electrochemical

oxidation and reduction take place in the high positive or negative potentials, that limits choice of suitable solvents and electrode materials.

Electrochemical reduction of bile acids is possible because of the present carboxyl group at C_{24} or C_{27}[12,20]. Free bile acids give pH independent peak at the potential from −1150 mV to –1350 mV, reduction of ursodeoxycholic acid takes place about 100 mV to more positive potentials. Similar behaviour can be observed with taurine and glycine conjugates. Differential pulse polarographic determination of cholic, deoxycholic, ursodeoxycholic, chenodeoxycholic and lithocholic acid at mercury dropping electrode was used to evidence the adsorption-desorption nature of electrode processes[12,21]. Polarographic maxima of oxygen (at −0.2 V) and zinc (at −1.2 V) were suppressed by selected C_{24} bile salts and used for the investigation of adsorptibility at micromolar concentrations, *i.e.* two orders of magnitude lower than CMC. Adsorption increases with rising number of hydroxyls.

Direct electrochemical oxidation of bile acids is hardly achievable and succeeds usually only in non-aqueous media or mixed media with minimal content of water[12]. Generally, cholesterol and its related compounds are directly oxidized at carbon based electrodes with lithium perchlorate supporting electrolyte[22]. The other approach relies on indirect oxidation by a mediator ion[23], which is a commonly used for oxidizing aliphatic hydroxyl groups with high oxidation potential. By indirect anodic electrochemical oxidation of cholic acids, whose hydroxyls were oxidized in this order C_7>C_{12}>C_3, various oxo-cholic acids were synthetized[23]. Later it was proved that the oxidation of cholesterol in acetonitrile at carbon fibre with glass cylinder electrode runs through a four-electron, four-proton transfer to cholesta-4,6-dien-3-one[24].

The alternative approach to detection of chromatographic methods in various biological matrices enables direct detection of cholesterol, without preceding derivatization and provide basis for development of a number of potential applications in detection of wide variety of steroid compounds[12]. After the selection of suitable components for the electrochemical flow cell in HPLC-ED (with electrochemical detection) at BDD electrode, the detection limit of cholesterol was 9 nmol·l^{-1} at detection potential of +2.2 V *vs.* an Ag/AgCl electrode, which is lower detection limit than for GCE and more usual HPLC-UV, LC/MS and LC/MS/MS methods. This method was used with methanol-acetonitrile-acetate buffer (c = 0.07 mol·l^{-1}, pH 5.0) mobile phase[25]. The electrochemical detector was composed of the control module and the analytical cell containing two inline porous carbon electrodes working with an oxidizing potential of +0.6 V and +1.4 V. The

results confirmed that this method is selective and sensitive enough for determining the UDCA and was much more sensitive in comparison with UV detection at 210 nm[25].

Another suitable method for the determination of bile acids is ion exchange chromatography with pulsed amperometric detection. Anionic phase at high pH is used and oxidation at gold working electrode, with sodium acetate mobile phase and hydrophobic stationary phase[26]. Although there are not many papers concerning electrochemical oxidation of bile acids, this way of detection appears to be the future of quick and cheap diagnosis.

3 Experimental

3.1 Studied analytes and reagents

Cholic acid (99.98 %, Sigma-Aldrich, Saint Louise, USA)

Chenodeoxycholic acid (99.98 %, Sigma-Aldrich, Saint Louise, USA)

Potassium hexacyanoferrate (II) trihydrate (Lach-Ner, Neratovice, Czech Republic)

Potassium chloride (Lachema, Brno, Czech Republic)

Deionized water (Milli-Qplus system, Millipore, USA)

Sulphuric acid (96 %, Lach-Ner, Neratovice, Czech Republic)

Acetonitrile (HPLC grade, Sigma-Aldrich, Saint Louise, USA)

Perchloric acid (70 %, Lach-Ner, Neratovice, Czech Republic)

Sodium perchlorate (anhydrous, HPLC grade, Fluka)

Silver nitrate (Ph. Eur. 3, Fluka)

Alumina (0.05 μm grain size, Elektrochemické detektory, Turnov, Czech Republic)

Stock solutions of the following substances were prepared: $1 \cdot 10^{-4}$ mol·l^{-1} CA in acetonitrile; $1 \cdot 10^{-3}$ mol·l^{-1} CDCA in acetonitrile; $1 \cdot 10^{-4}$ mol·l^{-1} $K_4[Fe(CN)_6] \cdot 3H_2O$ in 1 mol·l^{-1} KCl (aq); $1 \cdot 10^{-1}$ mol·l^{-1} H_2SO_4; 1 mol·l^{-1} $HClO_4$ in acetonitrile, All measured solutions were prepared in 10 ml calibrated voltammetric flasks, if not mentioned differently.

3.2 Apparatus, software and data analysis

Cyclic voltammograms were measured on EZStat Pro potentiostat (NuVant Systems, Crown Point, IN, USA) with its own software. The potentiostat PalmSense 4 (PalmSense BV, Houten, The Netherlands) was used primarily for differential pulse voltammetric measurements. These were performed under the Microsoft Windows XP Professional (Microsoft Corporation) operational system to data manipulation and to preview voltammograms. The results were further processed in OriginPro 8 (OriginLab Corporation, USA), Excel 2007 (Microsoft, USA), and Word 2007 (Microsoft, USA). All curves were measured at least 3 times, to create illustrative voltammetric figures usually the second scan was used.

Platinum auxiliary electrode (ETP CZ P 00506, Elektrochemické detektory, Turnov, Czech Republic) was used in three electrode system, along with silver / silver chloride reference electrode (EPP CZ R 00406, Elektrochemické detektory, Turnov, Czech Republic) in 3 $mol \cdot l^{-1}$ KCl (aq) and BDD working electrode for all measurements in aqueous media. Measurements of bile acids in mixed acetonitrile/water media were carried out in an electrochemical cell with special interspace (salt bridge), separating the working and reference electrode and containing 0.5 $mol \cdot l^{-1}$ $NaClO_4$ in acetonitrile, and Pleskov´s reference electrode (0.01 $mol \cdot l^{-1}$ $AgNO_3$ and 1 $mol \cdot l^{-1}$ $NaClO_4$ in acetonitrile)[27]. The following working disc electrodes were used: BDD (d = 3 mm, Windsor Scientific, Slough, UK), glassy carbon (d = 3 mm Radiometer Analytical SAS, Villeurbanne, France) and platinum (d = 2 mm, Radiometer Copenhagen, Denmark). The working electrodes were polished between each measurement for 4 minutes with slurry of alumina grain in distilled water on polishing pad (Elektrochemické detektory, Turnov Czech Republic) wiping with wood pulp when solutions containing bile acids were used.

3.3 Procedures and methods

3.3.1 Cyclic voltammetry

The parameters of cyclic voltammetry (CV) were as follows: 3s pretreatment at +400 mV, +400 mV start potential, +1800 mV final potential and 50 $mV \cdot s^{-1}$ scan rate, if not mentioned differently. The voltammograms were exported to Excel and extrapolated peak currents were found by subtracting the value of current of elongated baseline from measured peak current at the peak potential. The method was used for characterization of the BDD electrode with help of the redox pair $[Fe(CN)_6]^{3-/4}$ measured at different scan rates. These measurements were performed in 1 $mol \cdot l^{-1}$ KCl, as a supporting electrolyte. Anodic activation of BDD electrode was performed in 100 $mmol \cdot l^{-1}$ sulfuric acid at the potential E_{act} = +2400 mV for 10 min. 4-minute alumina polishing was also used as another type of activation.

Furthermore, cyclic voltammetry was used to study the oxidation of CA and CDCA, in a mixed media of acetonitrile with a 0.26 % content of water from perchloric acid (c = 100 $mmol \cdot l^{-1}$) supporting electrolyte.

3.3.2 Differential pulse voltammetry

The calibration dependences were measured by differential pulse voltammetry (DPV) with the following parameters: 3 s pretreatment at +400 mV, 400 mV start potential, +1800 mV final potential, scan rate 25 $mV \cdot s^{-1}$, +25 mV pulse height and pulse width of 70 ms, if not mentioned differently. The peak current of bile acids was found by analysing voltammograms in PalmSense 4 by subtracting fitted extrapolated five grade polynomial matching the supporting electrolyte baseline from maximum measured peak current at the peak potential. For further processing data were exported to OriginPro 8 and Excel 2007, where the calibration curve was built and its parameters were found. The DPV limit of detection (LOD) and limit of quantification (LOQ) values were obtained by measuring the least visible concentration ten times and finding the standard deviation *s* of peak currents. Then LOD and LOQ were calculated as a three times and ten times standard deviation of peak current divided by the slope of the particular linear calibration relationship.

4 Results and discussion

4.1. Electrochemical characterisation of BDD electrode

The study was initiated at the BDD electrode, with regard to the wider potential window in the anodic area, compared to platinum and glassy carbon. Cyclic voltammetry was used to characterize the BDD surface. The one electron exchanging redox marker 0.1 mmol·l^{-1} $[Fe(CN)_6]^{4-/3-}$ in 1 mol·l^{-1} KCl was used for this purpose, as it is frequently used due to high sensitivity to the condition of BDD electrode surface.

Different activation methods, like anodic 10-minute pretreatment with 0.1 mol·l^{-1} sulphuric acid at +2400 mV and 4-minute alumina polishing, were applied. Completely new inactivated, anodically activated, polished and four months old BDD electrode surface were measured at 10 – 500 mV·s^{-1} scan rate and compared by rendering peak current dependence on square root of scan rate. The trend line parameters for each activation, along with 50 mV·s^{-1} ΔE_p and I_{pa}/I_{pc} are presented in a table 4.1 (Tab. 4.2).

Tab. 4.3 Comparison of difference of anodic and cathodic peak potential ΔE_p and the ratio of anodic and cathodic peak current I_{pa}/I_{pc} at 50 mV·s^{-1} of 100 µmol·l^{-1} $[Fe(CN)_6]^{3-/4-}$ in 1 mol·l^{-1} KCl and parameters of peak current dependence on square root of the scan rate.

Type of activation	ΔE_p, mV	I_{pa}/I_{pc}	Slope, nA·s$^{1/2}$·mV$^{-1/2}$		Intercept, nA		Correlation coefficient R	
			Anodic	Cathodic	Anodic	Cathodic	Anodic	Cathodic
Before beginning	87.24	1.00	106.2 ± 1.3	-97.5 ± 2.1	171.6 ± 16.0	-211.5 ± 27.0	0.9989	0.9963
Anodic pretreatment (E_{act} = +2400 mV; t_{act} = 10 min)	221.37	1.17	104.9 ± 0.4	-65.1 ± 1.5	102.5 ± 4.4	-224.9 ± 19.5	0.9999	0.9957
After polishing (t = 4 min)	90.19	1.05	123.2 ± 3.2	-114.2 ± 3.7	168.9 ± 40.5	-175.5 ± 47.4	0.9987	0.9979
After four months	73.29	0.99	118.0 ± 1.1	-131.0 ± 0.9	108.7 ± 13.4	-40.3 ± 11.3	0.9994	0.9996

At the beginning, before all other experiments, the voltammetric response of $[Fe(CN)_6]^{4-/3-}$ on completely new, not activated BDD surface was measured (cyclic voltammograms see in Fig. 4.1). Quasi-reversible behaviour was observed and the difference of the anodic and the cathodic peak potential ΔE_p ranged from 80 mV to 200 mV, increasing with rising scan rate. For conventional reversible electrochemical processes applies 59 mV peak potential difference and the one-to-one ratio of cathodic and anodic peak currents. BDD met the second condition; the first one is rare in

case of solid electrodes. The peak currents increased linearly with square root of the scan rate (parameters in Tab. 4.4), which means the electrochemical process is controlled by diffusion.

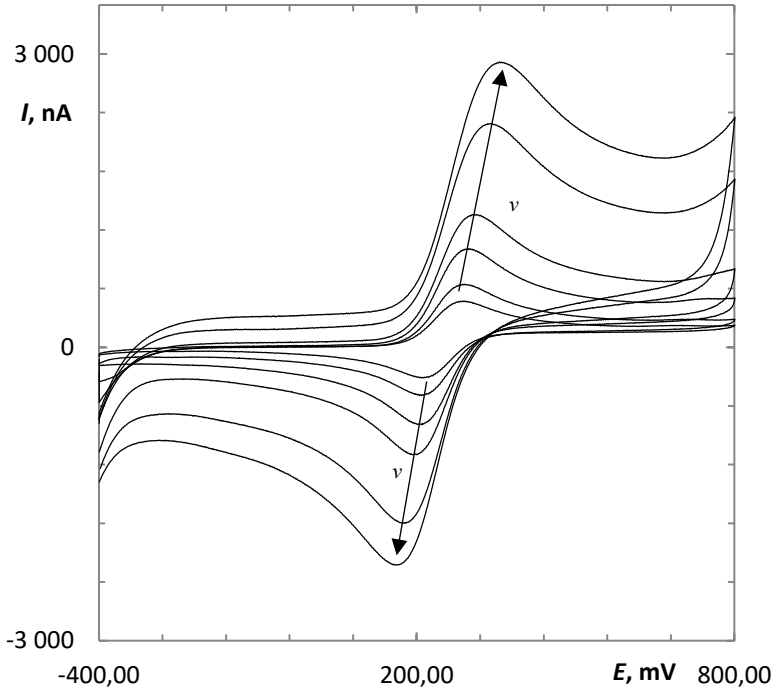

Fig. 4.1 Cyclic voltammograms of 100 μmol·l^{-1} $[Fe(CN)_6]^{3-/4-}$ in 1 mol·l^{-1} KCl at the beginning of all experiments on a new BDD electrode, scan rate v (mV·s^{-1}): (1) 10, (2) 20, (3) 50, (4) 100, (5) 300, (6) 500.

The next concern was to monitor an effect of 10-minute anodic activation at + 2400 mV (Fig. 4.2); 4-minute alumina polishing (Fig. 4.3); and final state of electrode after finishing of all experiments (Fig. 4.4); The figure 4.5 was created to better illustrate these differences on 50 mV·s^{-1} scan rate. Similar trends to figure 4.1 appear in peak potentials, their difference, peak currents and their ratio concerning increasing scan rate. In all cases dependence of peak current to square root of scan rate was rendered.

From these results we can clearly see that the anodic activation deteriorated reversibility parameters, as it leads to the highest ΔE_p. On the other hand, we observe increase in peak signal and decrease of ΔE_p after anodic activation with each alumina polishing. In comparison to inactivated electrode surface, polishing is more effective to increases the anodic peak currents than the cathodic. It seems that the electrode is in the best condition when used and polished with respect to the electron transfer kinetics of $[Fe(CN)_6]^{4-/3-}$. Importantly, no substantial changes in response was observed after four months of the measuring period.

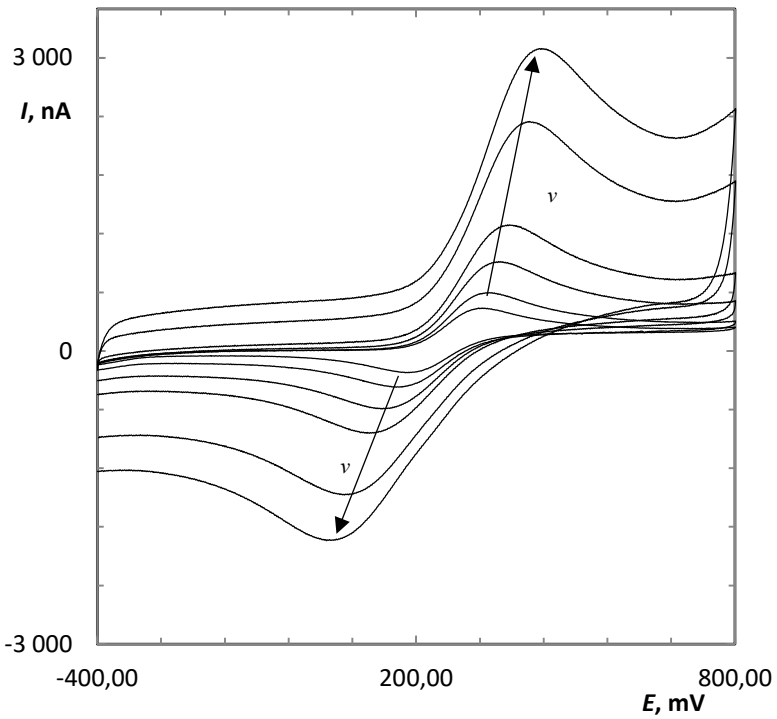

Fig. 4.2 Cyclic voltammograms of 100 µmol·l−1 $[Fe(CN)_6]3^{-/4-}$ in 1 mol·l^{-1} KCl after anodic activation in 0.1 mol·l^{-1} H_2SO_4, E_{act} = + 2400 mV for 10 minutes, scan rate (mV·s^{-1}): 10, 20, 50, 100, 300, 500.

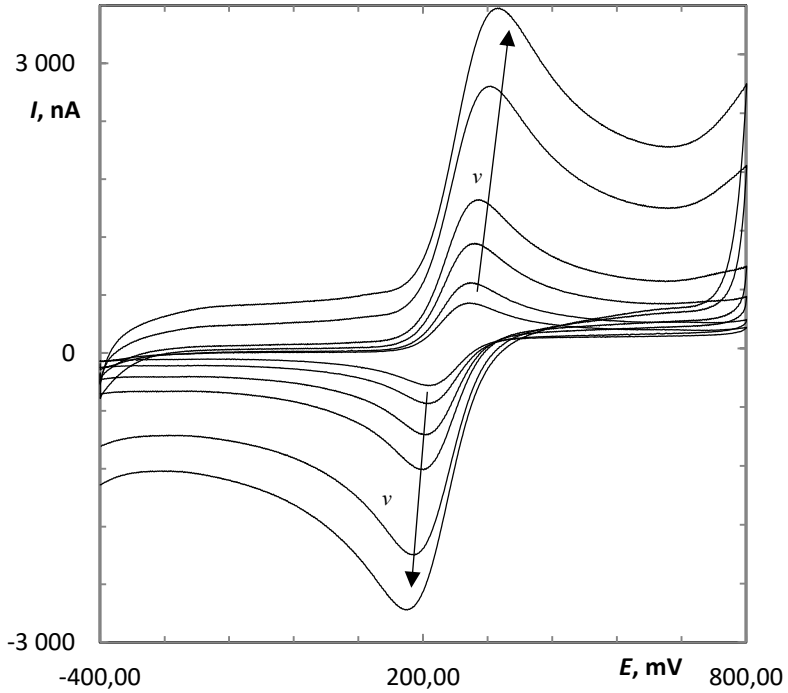

Fig. 4.3 Cyclic voltammograms of 100 µmol·l^{-1} $[Fe(CN)_6]^{3-/4-}$ in 1 mol·l^{-1} KCl after polishing of the surface of BDD electrode on alumina for 4 minutes, scan rate (mV·s^{-1}): 10, 20, 50, 100, 300, 500.

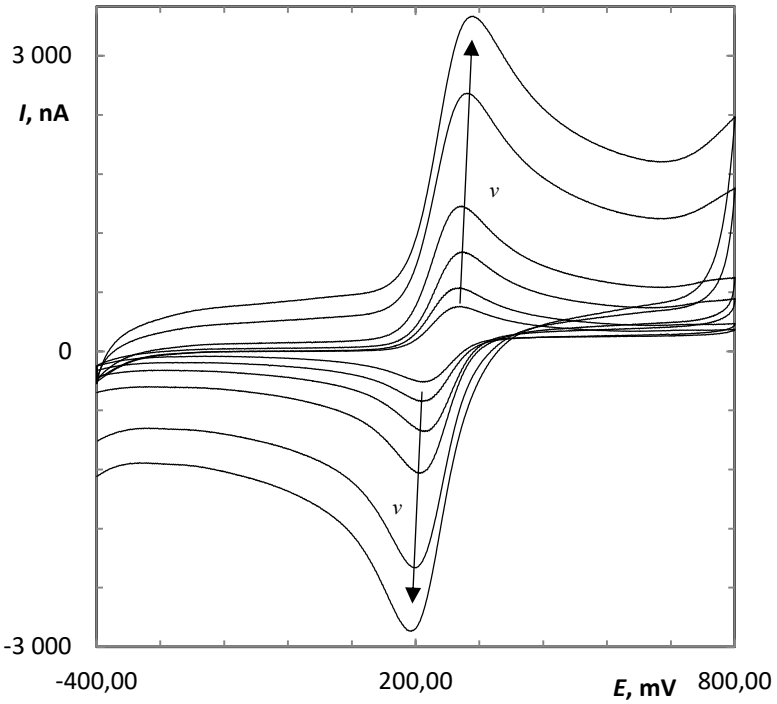

Fig. 4.4 Cyclic voltammograms of 100 μmol·l^{-1} $[Fe(CN)_6]^{3-/4-}$ in 1 mol·l^{-1} KCl after finishing whole experiment (4 months), scan rate (mV·s−1): 10, 20, 50, 100, 300, 500.

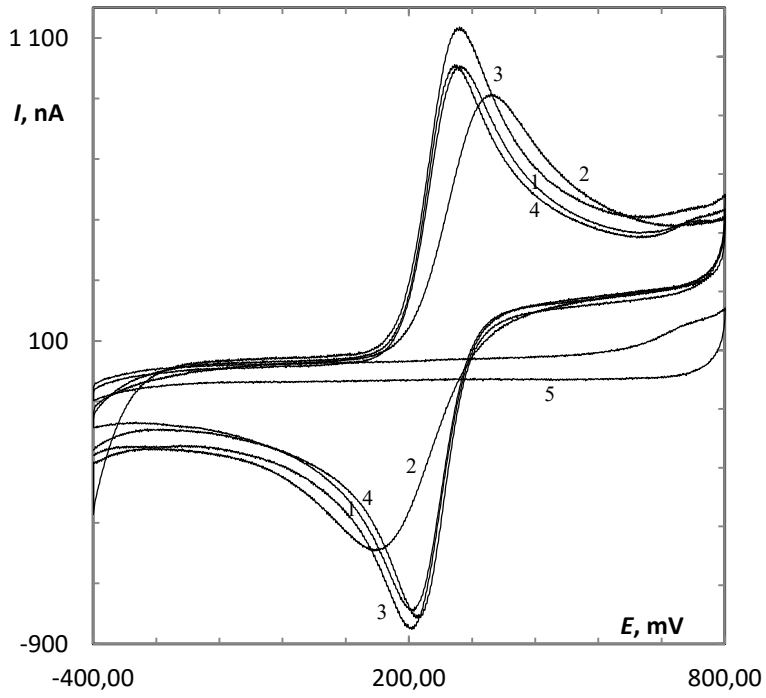

Fig. 4.5 Comparison of cyclic voltammograms of 100 μmol·l^{-1} $[Fe(CN)_6]^{3-/4-}$ in 1 mol·l−1 KCl on BDD electrode (1) before beginning of all experiments, (2) after anodic pretreatment, E_{act} = + 2400 mV for 10 minutes, (3) after polishing on alumina (4 min), (4) after finishing of all experiments, and (5) the supporting electrolyte. Scan rate: 50 mV·s^{-1}.

4.2. Cyclic voltammetry of CDCA and CA on BDD electrode

BDD electrode was further used for examination of electrochemical behaviour of studied analytes and their reaction mechanism by comparing voltammograms at different scan rates and observing change of signal with number of scans and effect of 10-second and 3-minute alumina polishing.

Cyclic voltammograms of CDCA and CA were measured in a mixed media of acetonitrile with a 0.26% content of water from perchloric acid (c = 0.1 mol·l^{-1}) used as the supporting electrolyte. Both analytes give first distinctive peak at about +1.1 V and second indistinctive one. Irreversible electrochemical process was observed for both bile acids. Cyclic voltammograms were measured at different scan rates, at initial 400 mV to final 1800 mV potential.

CDCA provides two anodic peaks at about +1100 mV and smaller one at about +1260 mV. The 100 μmol·l^{-1} solution of CDCA was measured at 10 – 100 mV·s^{-1} scan rate, where the potential of the most visible peak increased from +1094 to +1126 mV with increasing scan rate, as can be seen in Fig 4.6. CA provides two anodic peaks at about +1100 mV and smaller one at about +780 mV. The 100 μmol·l^{-1} solution of CA was measured at the scan rate of 10 – 500 mV·s^{-1}. The potential of the first, distinctive peak increases from +1089 to +1185 mV with increasing scan rate, as can be seen in Fig 4.7. The dependences of peak current on square root of scan rate are linear that indicates diffusion driven process. Their parameters are given in Tab. 4.2.

Tab. 4.2 Parameters of the peak current dependence on square root of the scan rate of 100 μmol·l^{-1} CA and CDCA in acetonitrile with 100 mmol·l^{-1} $HClO_4$ and 0.26 % H_2O

	Slope, μA$^{1/2}$·s$^{1/2}$·mV$^{-1/2}$	Intercept, μA	Correlation coefficient R
CA	2.16 ± 0.42	513.52 ± 110.27	0,9483
CDCA	2.96 ± 0.18	27.54 ± 10.41	0,9962

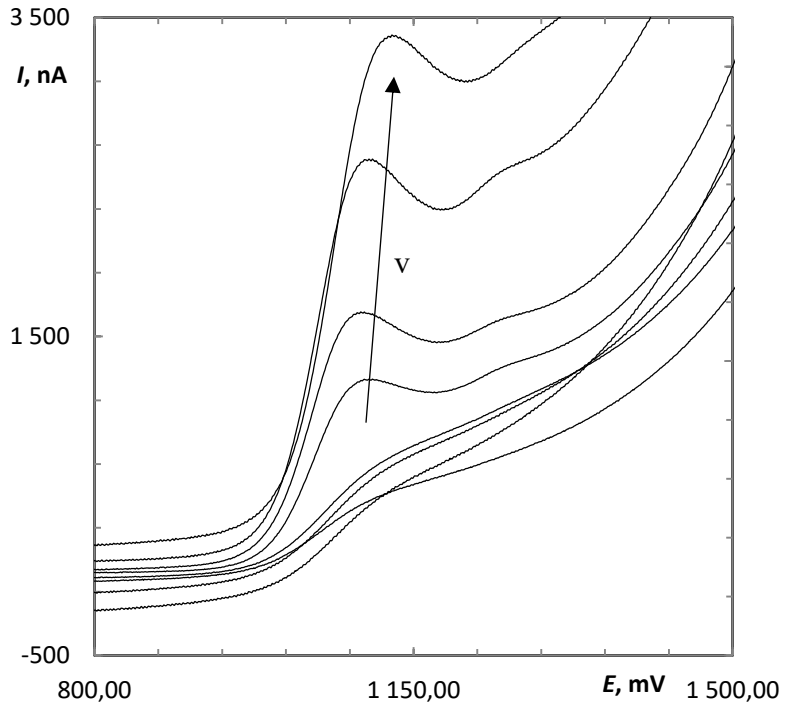

Fig. 4.6 Cyclic voltammograms of 100 μmol·l^{-1} CDCA in 100 mmol·l^{-1} $HClO_4$ in acetonitrile (water content 0.26 % H_2O), scan rate (mV·s^{-1}): 10, 20, 50, 100.

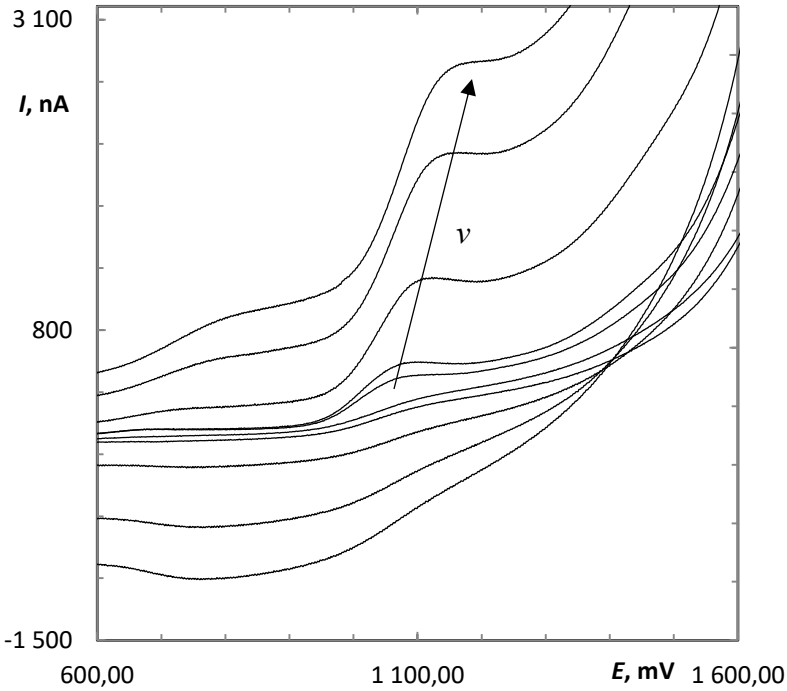

Fig. 4.7 Cyclic voltammograms of 100 μmol·l^{-1} CA in 100 mmol·l^{-1} $HClO_4$ in acetonitrile (water content 0.26 % H_2O), scan rate (mV·s^{-1}): 10, 20, 100, 300, 500.

The stability and repeatability of the voltammetric signal was also tested. It was found that in the first minutes after solution preparation the peak height is increasing in the time[28]. This trend

can be seen in Fig. 4.8, where in A there are 20 cyclic consecutive cyclic voltammograms and in B there is a peak current dependence on the number of cycles. The voltammetric response gets stabilized after approximately 80 min.

Further, the repeatability of voltammetric response of stabilized solution was investigated. After stabilizing of the solution, passivation is observed with increasing number of scans (Fig. 4.9). The peak current of CA during three consecutive cycles decreases from about 590 mV to 470 mV, which is more than 20 %.

To minimize the effect of passivation 10-second and 3-minute alumina polishing was applied between consecutive scans. To illustrate importance of polishing the solution of 50 μmol·l^{-1} CA on BDD electrode was measured using cyclic voltammetry. Always three scans were applied and then the BDD surface was polished. The values of peak current and potentials of the first two scans are statistically evaluated in the table 4.3 (Tab. 4.3). In the fig. 4.10 there are depicted the first scans of 3-minute polishing. The RSD value of peak currents of the first scan is 8.34 % that is lower than the RSD of first scans of 10-second polishing that is 13.78 %. Simultaneously higher peak currents were measured after 3-minute polishing. For the second scan of 3-minute polishing, the RSD valued 5.44 %. The second scans can be seen in Fig. 4.11. This figure also demonstrates that 3-minute polishing gives higher peak current with lower RSD value of I_p than 10-second polishing (RSD = 10.22 %). First scans of cholic acid are shown in the figure 4.12 during 10-second polishing. Peak currents and potentials are summarized in tab. 4.3. RDS of peak current of 10-second polishing is 13.78 % for the first scans which is comparable to 10.22 % for the second scans. The RSD of potentials ranged from 0.32% to 1.10 % around 1.168 V.

It was found that oxidation of CDCA and CA on BDD electrode is diffusion driven process and it undergoes passivation. The best repeatability was obtained by the second scan after 3-minute polishing, with smallest RSD.

Tab. 4.2 Statistical procession of peak currents I_p and potentials E_p of 50 μmol·l^{-1} CA measured using cyclic voltammetry in in 100 mmol·l^{-1} $HClO_4$ in acetonitrile (water content = 0.26 %) after 10-second and 3-minute polishing on alumina on BDD electrode and their statistical evaluation.

	3-minute alumina polishing				10-second alumina polishing			
	1. scan		2. scan		1. scan		2. scan	
	I_p, μA	E_p, V	I_p, μA	E_p, V	I_p, μA	E_p, V	I_p, μA	E_p, V
average	0.528	1.161	0.436	1.168	0.362	1.163	0.315	1.157
SD	0.044	0.005	0.024	0.008	0.050	0.013	0.032	0.004
RSD	8.343	0.445	5.443	0.700	13.783	1.103	10.215	0.326

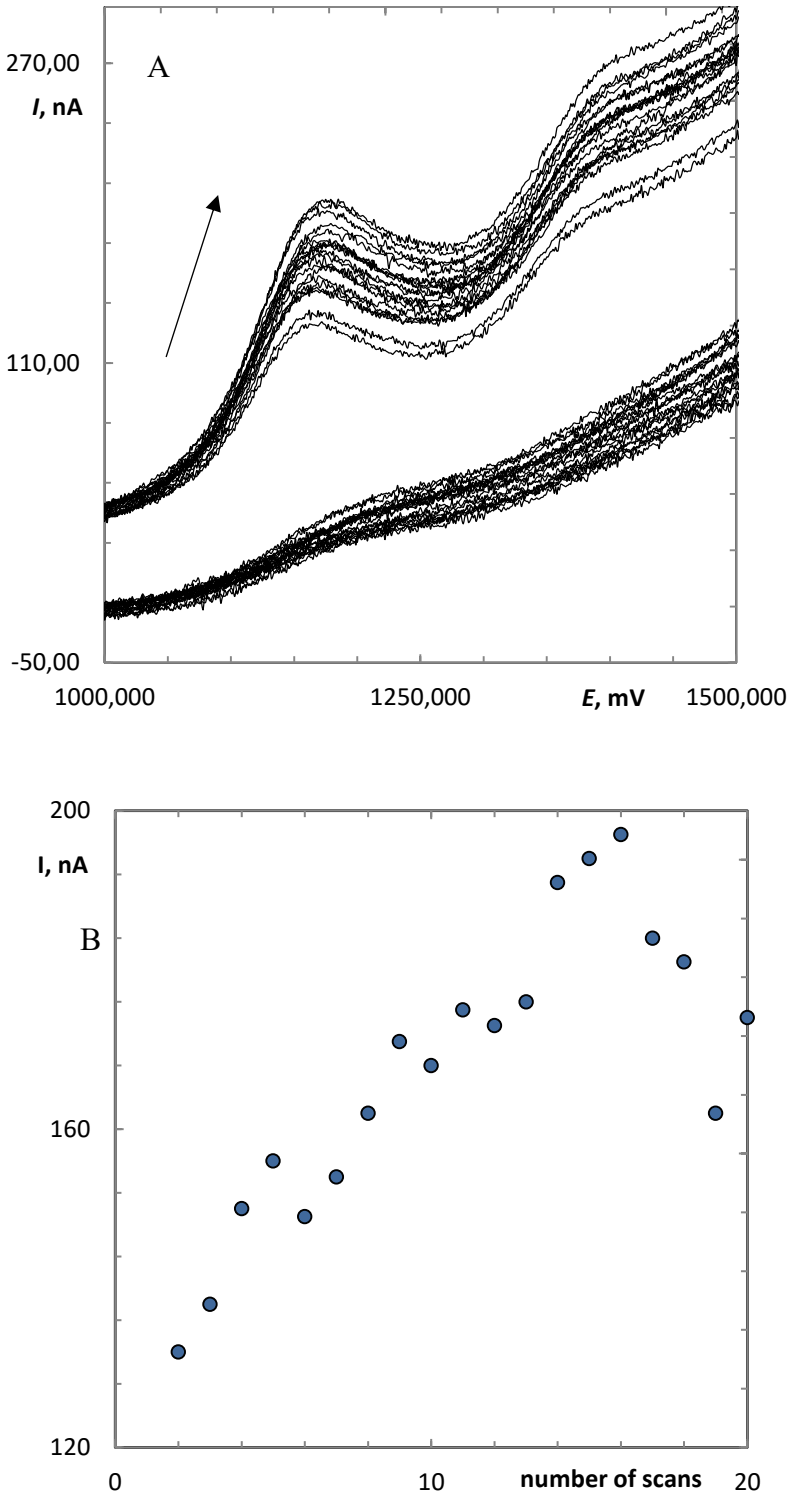

Fig. 4.8 (A) Twenty consecutive cyclic voltammograms of 50 μmol·l^{-1} CA in 100 mmol·l^{-1} $HClO_4$ in acetonitrile (water content = 0.26 %), recorded after preparation of the measured solution, scan rate 50 mV·s^{-1}, arrow shows increasing number of scans (B) Dependence of peak current *I* on the number of scans.

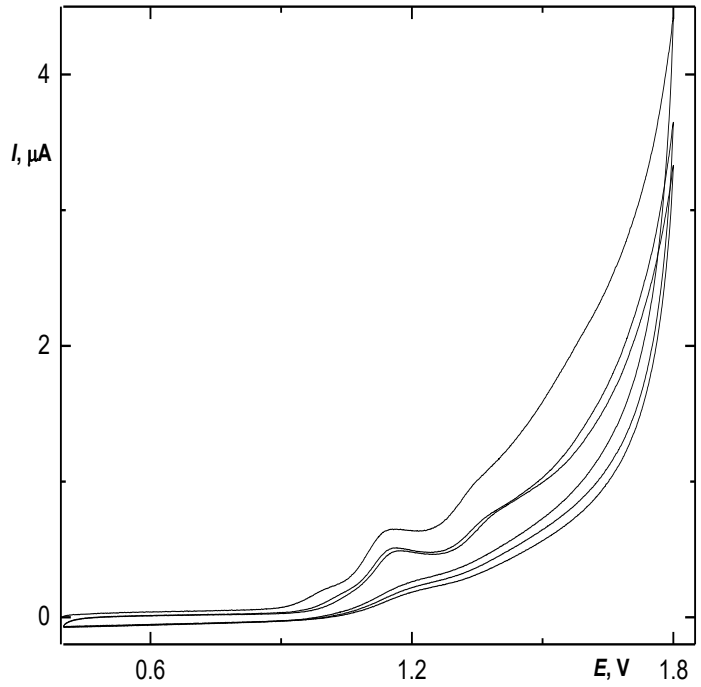

Fig. 4.9 Three consecutive cyclic voltammogram of 50 μmol·l^{-1} CA in 100 mmol·l^{-1} $HClO_4$ in acetonitrile (water content = 0.26 %), on BDD electrode after alumina polishing for 3 min. Scan rate 50 mV·s^{-1}.

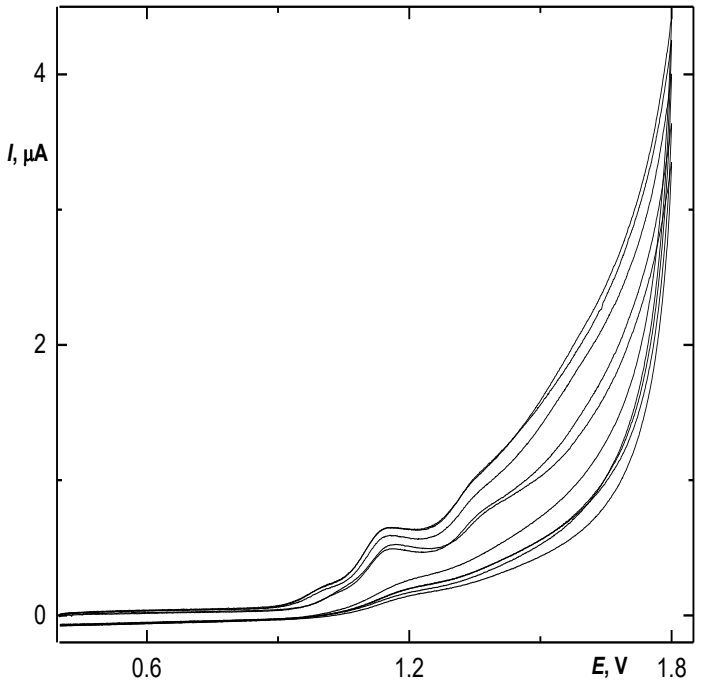

Fig. 4.10 The first scans of cyclic voltammograms of 50 μmol·l^{-1} CA in 100 mmol·l^{-1} $HClO_4$ in acetonitrile (water content = 0.26 %), on BDD electrode after alumina polishing for 3 min. Scan rate 50 mV·s$^{-,1}$, five repeated measurements.

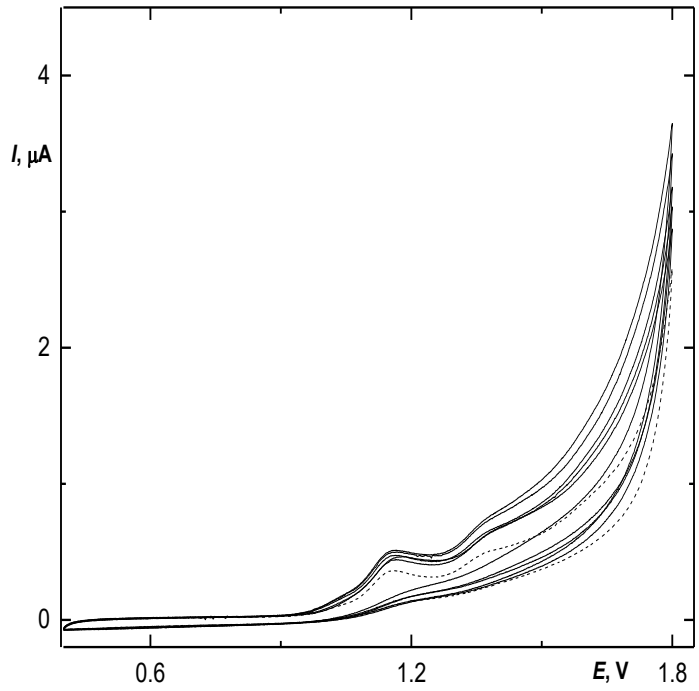

Fig. 4.11 The second scans of cyclic voltammograms of 50 μmol·l^{-1} CA in 100 mmol·l^{-1} $HClO_4$ in acetonitrile (water content = 0.26 %), on BDD electrode after alumina polishing for 3 min, compared to the lowest scan with 10 second polishing (dashed line). Scan rate 50 mV·s$^{-,1}$.

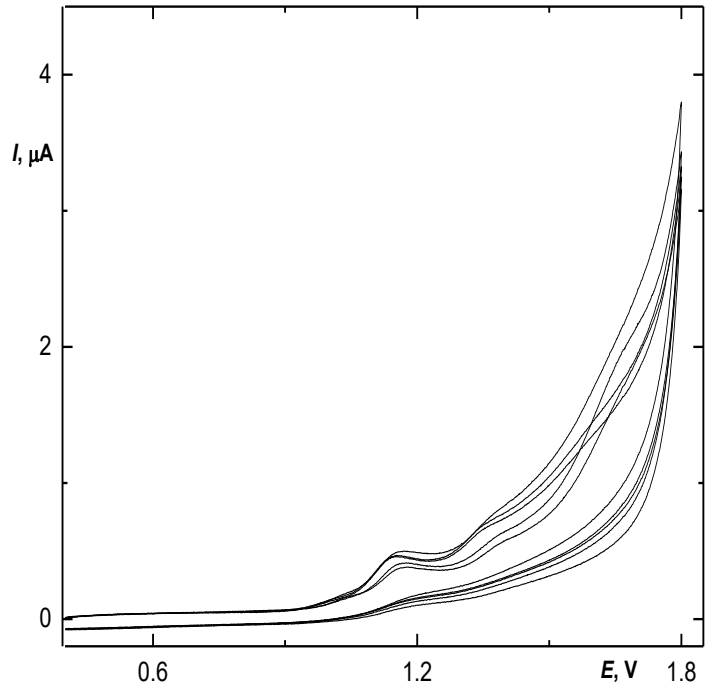

Fig. 4.12 The first scans of cyclic voltammograms of 50 μmol·l^{-1} CA in 100 mmol·l^{-1} $HClO_4$ in acetonitrile (water content = 0.26 %), on BDD electrode after alumina polishing for 10 seconds. Scan rate 50 mV·s$^{-,1}$, five repeated measurements

4.3 Calibration dependences

The calibration dependences were measured by DPV from +400 mV start potential to +1800 mV final potential with scan rate of 25 $mV.s^{-1}$. Chenodeoxycholic and cholic acids were measured in acetonitrile with 0.1 $mol \cdot l^{-1}$. $HClO_4$ and 0.26 % H_2O, at boron doped diamond, glassy carbon and platinum electrode. The comparison of voltammetric signals of 50 $\mu mol \cdot l^{-1}$ CDCA and CA on these three different electrodes is given in the table (Tab. 4.3), where peak potentials and current densities are listed. The illustrative voltammograms are in Fig. 4.10. It is obvious that voltammograms measured at the BDD electrode has greatest signal/background ratio. GCE electrode has the biggest current background. The CDCA at BDD electrode in mixed solution of acetonitrile gives two peaks at about +1.1 V and +1.4 V. This is very similar for the other two electrodes (GCE and PtE), but the potential window is narrower than in BDD, so the peaks at + 1.4 V peaks blur together in the onset of supporting electrolyte. In the case of CA, four peaks are observed at BDD electrode, at about +0.6 V, +1.0 V, +1.1 V, +1.4 V with the main one at +1.1 V. Signals measured at GCE appeared at +1.1 V and +0.9 V and at +1.1 V and +0.7 V using Pt electrode. Obviously, the material of the electrode and the presence of the extra 12α-hydroxyl group of CA influences the oxidation mechanism. Further studies are in progress to elucidate the reaction mechanism. However, the best visible peak with stable positioning and current was in all cases the peak at a +1.1 V and thus was further used for evaluation of calibration dependencies.

Tab. 4.3 Peak potentials and current densities of 50 $\mu mol \cdot l^{-1}$ CA and CDCA measured by DPV with 100 $mmol \cdot l^{-1}$ $HClO_4$ in acetonitrile (water content = 0.26 %), at boron doped diamond, glassy carbon and platinum electrode.

Electrode	E_{p1}, V	i_{p1}, $mA \cdot m^{-2}$	E_{p2}, V	i_{p2}, $mA \cdot m^{-2}$	E_{p3}, V	i_{p3}, $mA \cdot m^{-2}$	E_{p4}, V	i_{p4}, $mA \cdot m^{-2}$
Chenodeoxycholic acid								
BDD	1.14	38.97	1.38	6.46	-	-	-	-
GCE	1.12	69.01	1.34[a]	22.54	-	-	-	-
PtE	1.16	45.16	1.42[a]	11.97	-	-	-	-
Cholic acid								
BDD	1.13	18.89	1.36	51.44	1.02	16.52	0.63	1.60
GCE	1.12	16.97	[a]	[a]	0.87	12.06	-	-
PtE	1.16	20.65	[a]	[a]	-	-	0.66	8.25

[a] – poor signal, smaller potential window, sooner supporting electrolyte oxidation

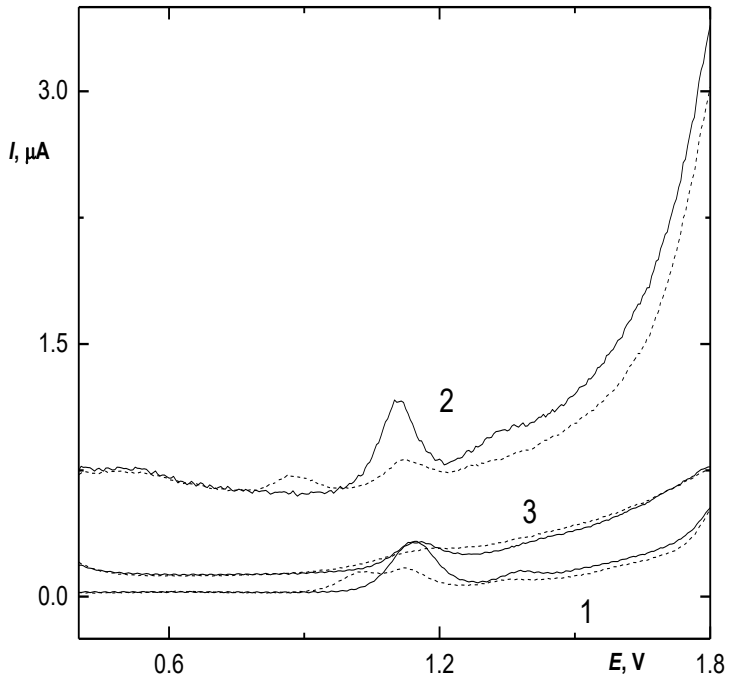

Fig. 4.10 DPV voltammograms of 50 μmol·l^{-1} CDCA (full lines) and CA (dotted lines) at BDD electrode (1), GCE (2) and PtE (3). Supporting electrolyte: 0.1 mol·l^{-1} $HClO_4$ and 0.26 % H_2O in acetonitrile.

The calibration dependencies of CDCA were measured in the concentration range of 1 – 900 μmol·l^{-1}. Calculated parameters of linear calibration dependences are given in Tab. 4.4 and corresponding voltammograms measured at BDD, GCE and PtE electrode are found in the figures Fig. 4.11, Fig. 4.12, Fig. 4.13, respectively. The linear dynamic range of CDCA was found over two concentration ranges. The slopes of CDCA calibration dependences were comparable for BDD electrode and GCE, the PtE has approximately half the slope. This lower value cannot be attributed only to lower electrode area (A = 3.1 mm^2 for PtE; A = 7.1mm^2 for BDD and GCE), but to lower sensitivity of the Pt electrode material to CDCA oxidation. Also the LOD is higher at PtE compared to GCE and BDD, which is caused by both, lower slope and worse repeatability of peak currents.

Tab. 4.4 Parameters of calibration dependence and limit of detection (LOD) and quantification (LOQ) of CDCA by DPV at BDD electrode, GCE and PtE electrode, concentration range of 5-900 μmol·l^{-1}. Supporting electrolyte 0.1 mol·l^{-1} $HClO_4$ and 0.26 % H_2O in acetonitrile.

Electrode	LDR, μmol·l^{-1}	Slope, μA·l·mol^{-1}	Intercept, μA	Correlation coefficient R	LOD, μmol·l^{-1}	LOQ, μmol·l^{-1}
BDD	5-900	4222.0 ± 122.2	0,09 ± 0,05	0.9930	5.3	17.6
GCE	5-900	5307.5 ± 328.8	0,24 ± 0,14	0.9705	5.1	16.9
PtE	10-900	2707.3 ± 15.2	-0,01 ± 0,01	0.9998	9.8	32.6

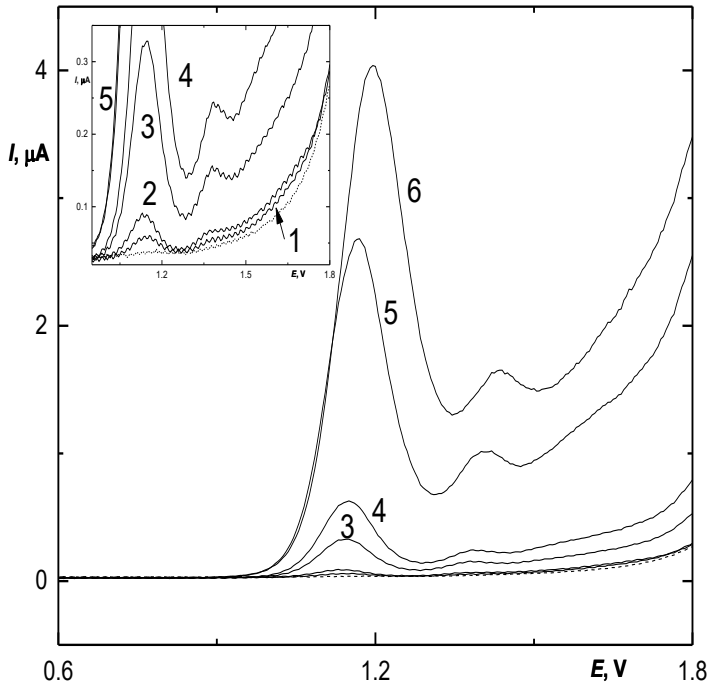

Fig. 4.11 DPV voltammograms of CDCA in acetonitrile with 0.1 mol·l^{-1} $HClO_4$ and 0.26 % H_2O at BDD working electrode. Concentrations of CDCA (μmol·l^{-1}): (1) 5, (2) 10, (3) 50, (4) 100, (5) 500, (6) 900. Dashed line shows the basic electrolyte.

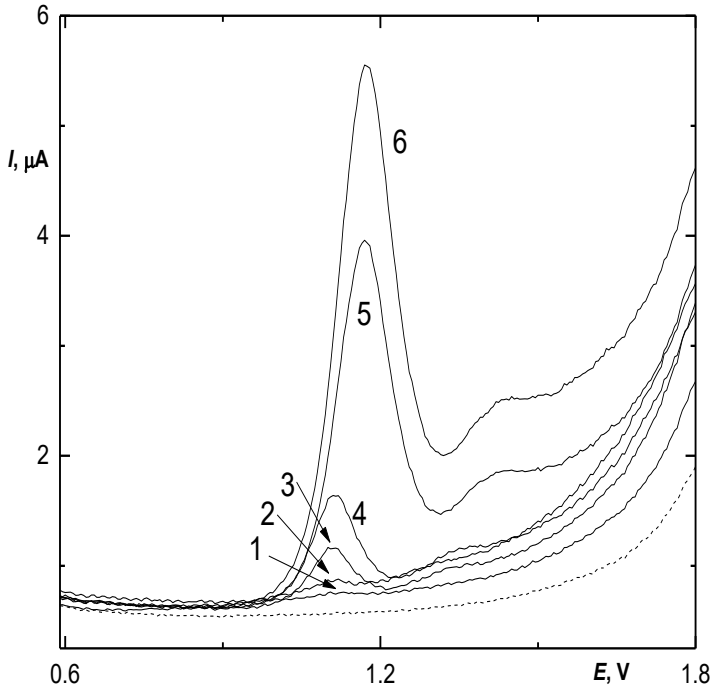

Fig. 4.12 DPV voltammograms of CDCA in acetonitrile with 0.1 mol·l^{-1} $HClO_4$ and 0.26 % H_2O, at GCE working electrode. Concentrations of CDCA (μmol·l^{-1}): (1) 5, (2) 10, (3) 50, (4) 100, (5) 500, (6) 900. Dashed line shows the basic electrolyte.

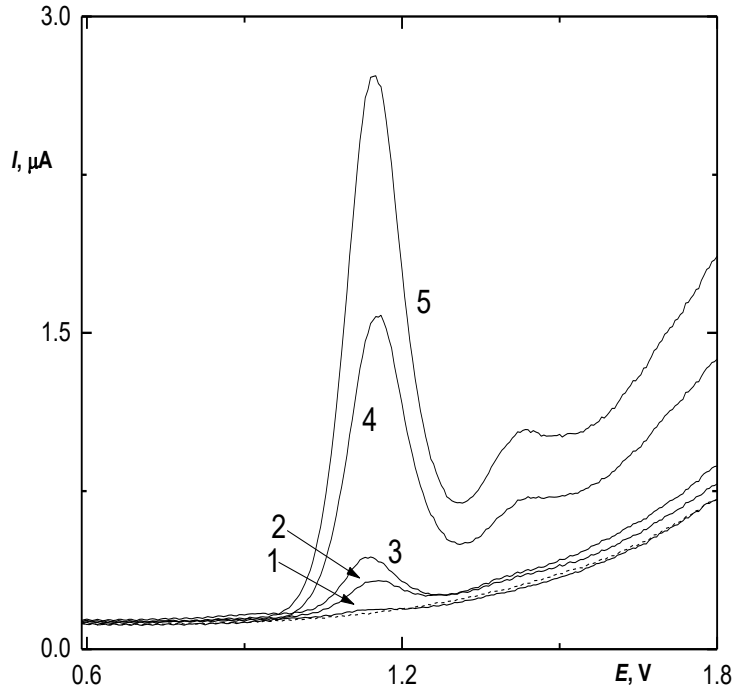

Fig. 4.13 DPV voltammograms of CDCA in acetonitrile with 0.1 mol·l^{-1} $HClO_4$ and 0.26 % H_2O, at Pt working electrode. Concentrations of CDCA (μmol·l^{-1} (1) 10, (2) 50, (3) 100, (4) 500, (5) 900. Dashed line shows the basic electrolyte.

The calibration dependencies of CA were measured in concentration range 1 - 90 μmol·l^{-1}. The parameters of linear calibration dependences were calculated for peak at 1.1 V and can be seen in Tab. 4.5. Corresponding voltammograms measured at BDD electrode, GCE, and Pt electrode are found in the figures Fig. 4.14, Fig. 4.15, Fig. 4.16 respectively. In general, the slopes of linear calibration dependency of CA are smaller than for CDCA. The slope is highest for BDD, GCE and PtE exhibit less than half the slope. Thus the lowest value of LOD was reached at BDD electrode. In spite of similar GCE and BDD electrode calibration slope, LOD at GCE is ten times higher. This can be explained by worse repeatability on GCE electrode.

Tab. 4.5 Parameters of calibration dependence of CA by DPV at BDD, GCE and PtE electrode, concentration range of 2.5-90 μmol·l^{-1}, with its limit of detection and quantification.

Electrode	LDR, μmol·l^{-1}	Slope, μA·l·mol^{-1}	Intercept, μA	Correlation coefficient R	LOD, μmol·l^{-1}	LOQ, μmol·l^{-1}
BDD	2.5-75	2074.4 ± 96.3	0.0 ± 0.0	0.9801	2.4	8.0
GCE	25-90	798.5 ± 394.5	0.1 ± 0.0	0.6076	112.1	373.7
PtE	10-90	724.5± 65.5	0.0 ± 0.0	0.9507	18.5	61.7

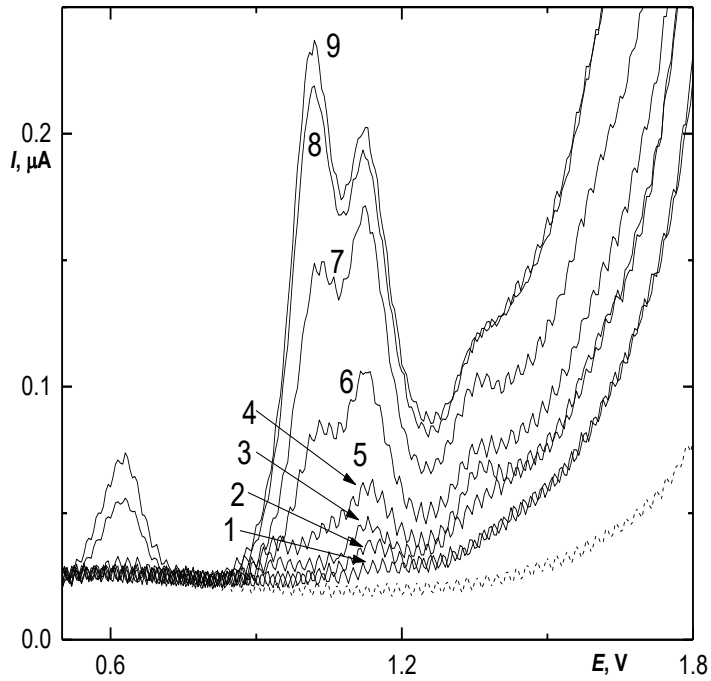

Fig. 4.14 DPV voltammograms of CA in acetonitrile with 0.1 mol·l^{-1} $HClO_4$ and 0.26 % H_2O, at BDD working electrode. Concentrations of CDCA (μmol·l^{-1} (1) 5, (2) 7.5, (3) 10, (4) 25, (6) 50, (7) 75, (8) 90. Dashed line shows the basic electrolyte.

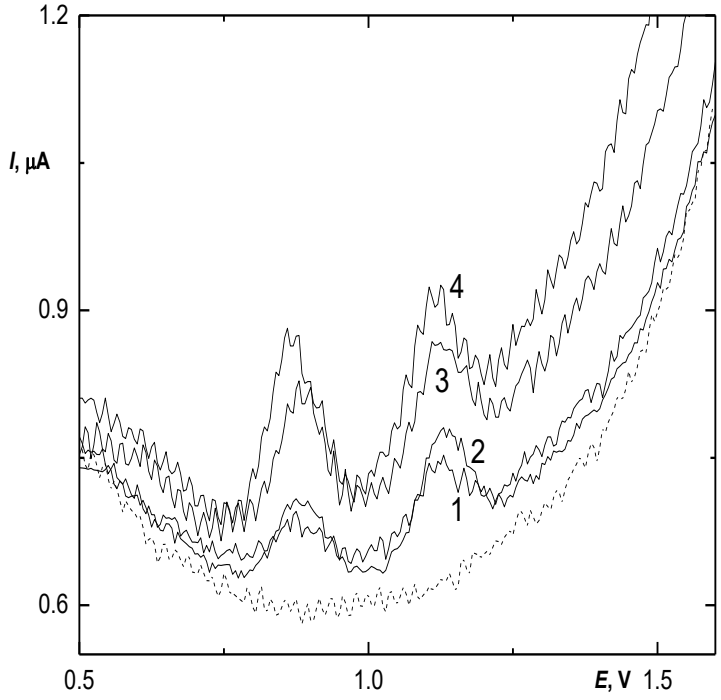

Fig. 4.15 DPV voltammograms of CDCA in acetonitrile with 0.1 mol·l^{-1} $HClO_4$ and 0.26 % H_2O, at GCE working electrode. Concentrations of CDCA (μmol·l^{-1}): (1) 25, (2) 50, (3) 75, (4) 90. Dashed line shows the basic electrolyte.

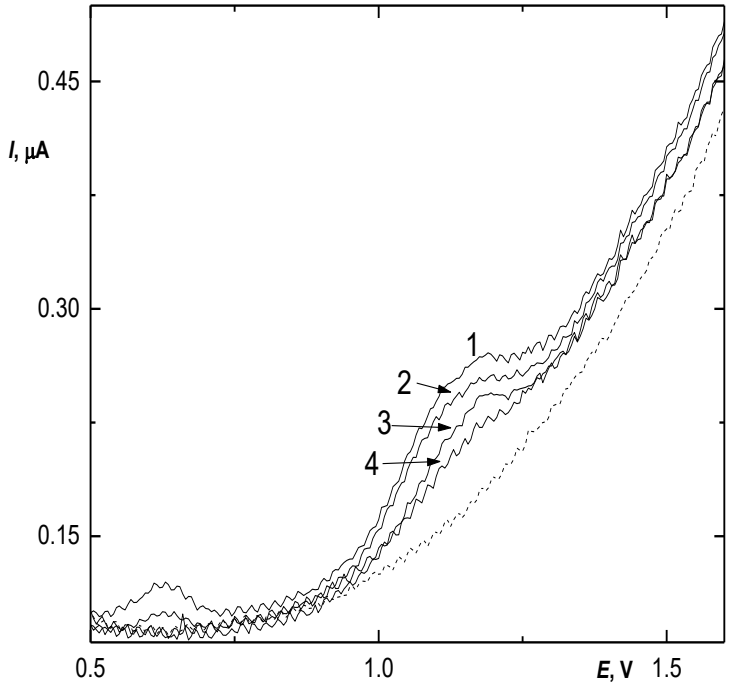

Fig. 4.16 DPV voltammograms of CDCA in acetonitrile with 0.1 mol·l^{-1} $HClO_4$ and 0.26 % H_2O, at PtE working electrode. Concentrations of CDCA (μmol·l^{-1}): (1) 25, (2) 50, (3) 75, (4) 90. Dashed line shows the basic electrolyte.

5 Conclusion

The concentration of bile acids is an important parameter in hepatobiliary tract diseases. To determine bile acids, mainly HPLC with different detectors (MS, MS-MS, TLC, ED) is used today, which could be preceded by derivatization, or radioimmunoassay, with risk of contamination. Due to this problem, there is a need to find simpler methods with rapid preparation methods, lower price, and higher sensitivity. Electrochemical detection is one of the relatively unexploited possibilities. According to our preliminary experiments, electrochemical oxidation of selected bile acid takes place in highly positive potentials in acetonitrile supporting electrolyte, similarly to cholesterol and other steroids.

This work deals with the electrochemical oxidation of the CDCA and CA at BDD electrode in comparison with the oxidation of glassy carbon and platinum in acetonitrile, or in a mixed media of acetonitrile and water.

The study was initiated at the BDD electrode, with regard to the wider window in the anodic area, compared to platinum, and glassy carbon. By cyclic voltammetry Characterization of the BDD electrode using a redox marker $[Fe(CN)_6]^{4-/3-}$ (c = 0.1 mmol·l^{-1}) in 1 mol·l^{-1} KCl, revealed quasi-reversible behaviour and the difference of the anodic and the cathodic peak potential ranged about 90 mV depending on the scan rate for alumina-polished BDD surface. 3 minute polishing by alumina was compared with 10 seconds polishing and anodic activation at + 2.4 V in 0.5 mol.l^{-1} sulphuric acid. Polishing the electrode surface of alumina was then applied to activate electrode surface between consecutive voltammetric scans in the presence of CA and CDCA.

CDCA and CA provides anodic peaks solutions in acetonitrile-water (0.26%) media containing 0.1 mol·l^{-1} $HClO_4$ as supporting electrolyte at all tested electrode materials. The oxidation for CDCA occurs in the relatively high potentials of about +1100 ± 100 mV, depending on the scan rate and used voltammetric technique. CA provides voltammetric response at lower potentials of ca +0.6 V. This observation was noted only in CA and CDCA, both of which contain 7-α-hydroxy group. Other tested bile acids did not provide any similar signal. The irreversibility of the process was proved by the absence of cathodic peak, even at the higher number of cycles. According to the relationship of current to square root of scan speed can be seen that the oxidation process is controlled by diffusion and smallest RSD, best repeatability has second scan of 3-minute polishing.

The calibration relationships were measured at a concentrations range of 1 – 900 μmol·l^{-1} for CDCA, and 1 - 90 μmol·l^{-1} for CA. They are linear and reach higher sensitivity at BDD in comparison to GC and Pt electrodes. The lowest value of LOD was reached for both CDCA and CA at BDD electrode. This can be explained by worse repeatability on GCE electrode and PtE.

From the results it is evident that only two primary bile acid, CDCA and CA, are oxidizable in an acetonitrile environment, with minimal addition of water, at the BDD electrode, platinum electrode and the electrode of glassy carbon. Further studies will be devoted to the oxidation mechanism and the possibility of its use for selective detection of these bile acids.

References

(1) Hofmann, A. F.; Hagey, L. R. Key Discoveries in Bile Acid Chemistry and Biology and Their Clinical Applications: History of the Last Eight Decades. *J. Lipid Res.* **2014**, *55* (8), 1553–1595.

(2) Wieland, H. *The Chemistry of the Bile Acids*; Elsevier Publishing Company, Amsterdam, The Netherlands, 1928.

(3) Bernal, J. Crystal Structures of Vitamin D and Related Compounds. *Nature* **1932**, 277–278.

(4) Lindley, P.; Carey, M. Molecular Packing of Bile Acids: Structure of Ursodeoxycholic Acid. *J. Crystallogr. Spectrosc.* **1987**, 231–249.

(5) Bergstrom, S.;Danielsson, H.; Samuelsson, B. Formation and Metabolism of Bile Acids. *Lipide Metab.* **1960**, 291–336.

(6) Norman, A.; Sjovall, J. On the Transformation and Enterohepatic Circulation of Cholic Acid in the Rat. *J. Biol. Chem.* **1958**, *233*, 872–885.

(7) Lindstedt, S. The Turnover of Cholic Acid in Man.* Bile Acids and Steroids 51. *Acta Physiol. Scand.* **1957**, *40* (1), 1–9.

(8) Nakayama, F. *Cholelithiasis: Causes and Treatment*; Igaku-Shoin Medical Pub, 1997.

(9) Mukhopadhyay, S.; Maitra, U. Chemistry and Biology of Bile Acids. *Curr. Sci.* **2004**, *87* (12), 1666–1683.

(10) De Aguiar Vallim, T. Q.; Tarling, E. J.; Edwards, P. A. Pleiotropic Roles of Bile Acids in Metabolism. *Cell Metab.* **2013**, *17* (5), 657–669.

(11) Hofmann, A. F.; Sjövall, J.; Kurz, G.; Radominska, A.; Schteingart, C. D.; Tint, G. S.; Vlahcevic, Z. R.; Setchell, K. D. A Proposed Nomenclature for Bile Acids. *J. Lipid Res.* **1992**, *33* (4), 599–604.

(12) Pecková, K.; Nesměrák, K. Electrochemistry of Bile Acids, Cholesterol, and Related Compounds. In *Sensing in Electroanalysis (Kalcher K., Metelka R., Švancara I., Vytřas K., eds.)*; University Press Centre, Pardubice, 2012; Vol. 7, pp 87–96.

(13) DrugBank (online). Canadian institutes of health, 2017 (accessed Mar 1, 2017) at https://www.drugbank.ca/drugs/.

(14) Roda A., Hofmann A. F., M. K. J. The Influence of Bile Salt Structure on Self-Association in Aqueous Solutions. *J. Biol. Chem.* **1983**, *258* (10), 6362–6370.

(15) Zhang, X.; Zhu, M.; Xu, B.; Cui, Y.; Tian, G.; Shi, Z.; Ding, M. Indirect Electrochemical

Detection for Total Bile Acids in Human Serum. *Biosens. Bioelectron.* **2016**, *85*, 563–567.

(16) Scalia, S. Bile Acid Separation. *J. Chromatogr. B Biomed. Sci. Appl.* **1995**, *671* (1–2), 299–317.

(17) Ye, L.; Liu, S.; Wang, M.; Shao, Y.; Ding, M. High-Performance Liquid Chromatography-Tandem Mass Spectrometry for the Analysis of Bile Acid Profiles in Serum of Women with Intrahepatic Cholestasis of Pregnancy. *J. Chromatogr. B Anal. Technol. Biomed. Life Sci.* **2007**, *860* (1), 10–17.

(18) Wu, Y.; Wang, X.; Wu, Q.; Wu, X.; Lin, X.; Xie, Z. Separation and Determination of Structurally Related Free Bile Acids by Pressurized Capillary Electrochromatography Coupled to Laser Induced Fluorescence Detection. *Anal. Methods* **2010**, *2* (12), 1927.

(19) Klouda Jan, Barek Jiří, Nesměrák Karel, S.-P. K. Non-Enzymatic Electrochemistry in Characterization and Analysis of Steroid Compounds. **2017**.

(20) Ferri, T.; Campanella, L.; De Angelis, G. Differential-Pulse Polarographic Determination of Cholic Acids. *Analyst* **1984**, *109* (7), 923.

(21) Milberg, C.; Kratohvil, J. P.; Zuman, P. Surface Orientation of Cholanoic Acids from Suppression of Polarographic Maxima. *J. Colloid Interface Sci.* **1988**, *126* (1), 63–68.

(22) Hojo, K.; Hakamata, H.; Kusu, F. Simultaneous Determination of Serum Lathosterol and Cholesterol by Semi-Micro High-Performance Liquid Chromatography with Electrochemical Detection. *J. Chromatogr. B Anal. Technol. Biomed. Life Sci.* **2011**, *879* (11–12), 751–755.

(23) Medici, A.; Pedrini, P.; De Battisti, A.; Fantin, G.; Fogagnolo, M.; Guerrini, A. Anodic Electrochemical Oxidation of Cholic Acid. *Steroids* **2001**, *66* (2), 63–69.

(24) Hosokawa, Y. Y.; Hakamata, H.; Murakami, T.; Aoyagi, S.; Kuroda, M.; Mimaki, Y.; Ito, A.; Morosawa, S.; Kusu, F. Electrochemical Oxidation of Cholesterol in Acetonitrile Leads to the Formation of Cholesta-4,6-Dien-3-One. *Electrochim. Acta* **2009**, *54* (26), 6412–6416.

(25) Scalia, S.; Tirendi, S.; Pazzi, P.; Bousquet, E. Assay of Free Bile Acids in Pharmaceutical Preparations by HPLC with Electrochemical Detection. *Int. J. Pharm.* **1995**, *115* (2), 249–253.

(26) Chaplin, M. F. Analysis of Bile Acids and Their Conjugates Using High-pH Anion-Exchange Chromatography with Pulsed Amperometric Detection. *J. Chromatogr. B Biomed. Sci. Appl.* **1995**, *664* (2), 431–434.

(27) Klouda, J. *Elektrochemická Oxidace Žlučových Kyselin Na Elektrodách Na Bázi Uhlíku. Možnosti Využití v Elektroanalýze. Bakalářská Práce.*; Charles University, Faculty of Science, 2015.

(28) Schwarzová-Pecková Karolina, Benešová Lenka , Habániková Shannelle Diana, Yershova Polina, K. J. *Possibilities of Electrochemical Oxidation of Sterols at Bare Electrode Materials*; In XXXVII. Modern Electrochemical Methods, Jetrichovice, 15.-19.5. **2017**; Navratil, T., Fojta, M., Schwarzová, K. Eds.; Best Servis: Usti nad Labem, 2017; in press.